NATIONAL ENERGY TECHNOLOGY LABORATORY
OIL & GAS

DOE Award No.: DE-FE0028973

Quarterly Research Performance Progress Report

(Period Ending 03/31/2017)

Advanced Simulation and Experiments of Strongly Coupled Geomechanics and Flow for Gas Hydrate Deposits: Validation and Field Application

Project Period (10/01/2016 to 09/30/2019)

Submitted by:
Jihoon Kim

_____
Signature

The Harold Vance Department of Petroleum Engineering,
College of Engineering
Texas A&M University
407K Richardson Building
3116 College Station TX, 77843-3136
Email: jihoon.kim@tamu.edu
Phone number: (979) 845-2205

Prepared for:
United States Department of Energy
National Energy Technology Laboratory

March 28, 2017

U.S. DEPARTMENT OF ENERGY | NATIONAL ENERGY TECHNOLOGY LABORATORY

Office of Fossil Energy

DISCLAIMER

TABLE OF CONTENTS

ACCOMPLISHMENTS

Objectives of the project

The objectives of the proposed research are (1) to investigate geomechanical responses induced by depressurization experimentally and numerically; (2) to enhance the current numerical simulation technology in order to simulate complex physically coupled processes by depressurization and (3) to perform in-depth numerical analyses of two selected potential production test sites: one based on the deposits observed at the Ulleung basin UBGH2-6 site; and the other based on well-characterized accumulations from the westend Prudhoe Bay. To these ends, the recipient will have the following specific objectives:

1). Information obtained from multi-scale experiments previously conducted at the recipient's research partner (the Korean Institute of Geoscience and Mineral Resources (KIGAM)) that were designed to represent the most promising known Ulleung Basin gas hydrate deposit as drilled at site UBGH2-6 will be evaluated (Task 2). These findings will be further tested by new experimental studies at Lawrence Berkeley National Laboratory (LBNL) and Texas A&M (TAMU) (Task 3) that are designed capture complex coupled physical processes between flow and geomechanics, such as sand production, capillarity, and formation of secondary hydrates. The findings of Tasks 2 and 3 will be used to further improve numerical codes.

2) Develop (in Tasks 4 through 6) an advanced coupled geomechanics and non-isothermal flow simulator ($T+M^{AM}$) to account for large deformation and strong capillarity. This new code will be validated using data from the literature, from previous work by the project team, and with the results of the proposed experimental studies. The developed simulator will be applied to both Ulleung Basin and Prudhoe Bay sites, effectively addressing complex geomechanical and petrophysical changes induced by depressurization (e.g., frost-heave, strong capillarity, cryo-suction, induced fracturing, and dynamic permeability).

Accomplished

The plan of the project timeline and tasks is shown in Table 1, and the activities and achievements during the second quarter of 2017 are listed as follows.

Task 1: Project management and planning

The first quarterly report and the project budget information (SF-424A) were submitted, revised, and re-submitted to NETL. All the participants of TAMU, LBNL, and KIGAM started this projects.

Task 2: Review and evaluation of experimental data of gas hydrate at various scales for gas production of Ulleung Basin

Subtask 2.1 Evaluation of Gas hydrate depressurization experiment of 1-m scale

We (KIGAM) are reviewing the 1D 1-m scale GH production experimental system already conducted previously as well as the corresponding data. We inspected our 1D 1-m scale GH production experimental system which includes high pressure cell, data acquisition equipment, fluid injection equipment, and temperature control equipment. After confirming that there was no leakage of pressure during the inspection, we packed sediment sample into the meter-scale pressure cell. The packed sediments consisted of alternate layers of clay-sand-clay representing the layering system in the Ulleung Basin geological structure. We also used artificial particles that mimic the grain size distribution of sandy layers found in the Ulleung Basin.

Subtask 2.2 Evaluation of Gas hydrate depressurization experiment of 10-m scale

Not initiated (future year tasks)

Subtask 2.3 Evaluation of Gas hydrate depressurization experiment of 1.5-m scale system in 3D

Not initiated (future year tasks)

Subtask 2.4 Evaluation of gas hydrate production experiment of the centimeter-scale system

We (KIGAM) revisited the experimental study on core-scale permeability measurements according to hydrate saturations, in order to make use of numerical simulation. In the experiment, we took specimens, choosing artificial samples and measuring porosity, of 98% SiO2 of HAMA#5, 6, 7, 8 (grain density=2.68g/㎤, mean particle size 106~774 ㎛). Porosity of HAMA #5, 6, and 8 ranges from 0.39 to 040, while that of HAMA #7 is 0.43, shown in Fig. 2.1. We measured permeability with different hydrate saturation, ranging from 0.05 to 0.2 and pre-processed the data for numerical simulation.

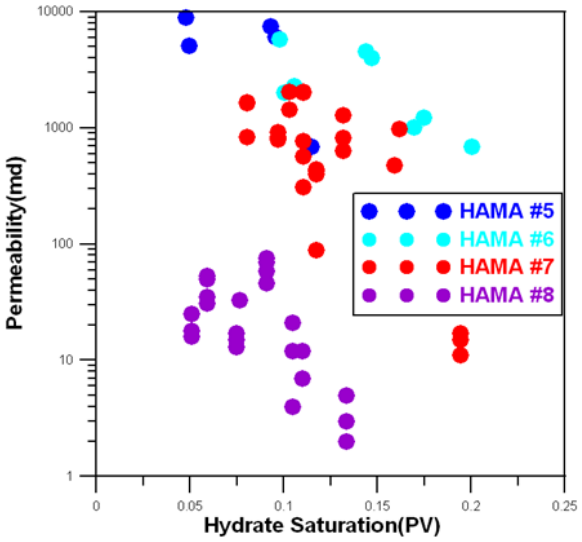

Fig. 2.1 Permeability vs. Hydrate saturation for different grain sizes.

Task 3: Laboratory Experiments for Numerical Model Verification

Subtask 3.1: Geomechanical changes from effective stress changes during dissociation

LBNL has been waiting for a larger X-ray transparent pressure vessel with multiple feed-throughs for this test. The vessel was ordered under another hydrate project in which it will be used as well, but is preferential to the existing vessel for these test. The vessel was improperly constructed, and rejected by the manufacturer. A new vessel is set to be completed in March 2017, pressure tested in April 2017, and delivered to LBNL. This does not impact project schedule at this point.

Subtask 3.2 Geomechanical changes from effective stress changes during dissociation – sand

Production

Not initiated

Subtask 3.3 Geomechanical changes resulting from secondary hydrate and capillary pressure

Changes

A new laboratory setup is developed at the TAMU hydrate laboratory to effectively measure the formation and dissociation of the hydrates in pore space. This setup will be used to study secondary hydrate and capillary pressure changes. As shown in the dissected diagram along with the dimensions and the sizes of the parts in Fig. 3.1, a stainless steel cylinder was divided into two main sections. Section A, pore-space, and Section B, empty-space filled with liquid. The apparatus consisted of three thermocouples in Section A. Measurement points and locations are circled in Fig. 3.3. One transducer was placed to measure the pore pressure P_1 in Section A and

another transducer to measure pressure P_2 in Section B. Methane was supplied to the pore-space. A simple schematics for the experimental setup is shown in Fig. 3. 2. Quartz sands were used for the experiment porous medium. The sieve analysis of the sand used is shown in Fig. 3.3.

Experimental sands were packed into the cylinder in Section A. For the experiment, 1,200cm^3 of sands with 36.2% porosity, determined by the water saturation method, was saturated 50% with filtered water. Methane gas was then injected and flushed twice around 100 bar (about 18,500 cm^3 of methane injected in 217.2cm^3 pore-space) to remove air inside the cylinder. After flushing the pore-volume, the cylinder was pressurized with methane up to 103 bar in Section A. The final methane injection resulted 50% water saturation and 50% gas saturation in the pore-volume in section A. Then the sands in cylinder was confined by pumping the water into Section B up to 300 bar using the water pump until the piston separating the two sections stopped being displaced.

The experiments will be conducted by first pressurizing the cylinder with water saturated sands to 103 bar at a room temperature, then the temperature-controlled chamber will be cooled to 1℃, a hydrate forming temperature without triggering the ice formation. Then the system was kept in 1℃ for at least 12 hours to observe the onset of hydrate formation, characterized by the exothermic reaction leading to localized temperature increase on the thermocouple. Once the hydrate formation stopped, the system was heated to a non-hydrate forming temperature to melt the hydrates in the system. Subsequent experiments will be conducted by only changing the temperature initial temperature to observe secondary hydrate formation conditions; no depressurization will be done.

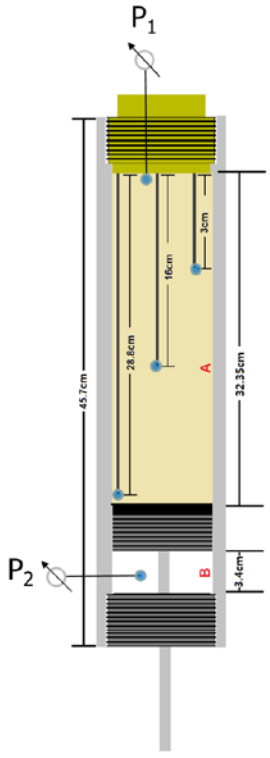

Fig. 3.1: Dissected diagram of the stainless steel cylinder to be used for Subtask 3.3 at TAMU hydrate laboratory.

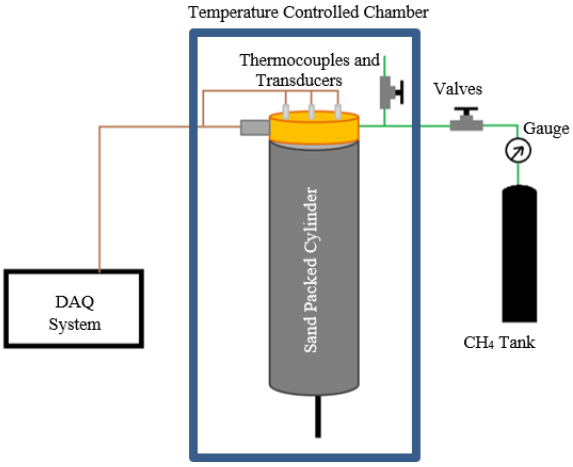

Fig. 3.2: Simple schematic of the laboratory setup for Subtask 3.3 at TAMU hydrate laboratory.

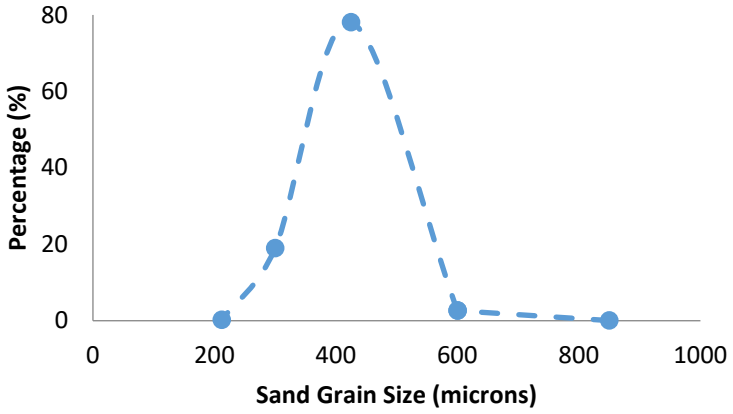

Fig. 3.3: Sieve analysis of beads sands (quartz) used for Subtask 3.3 at TAMU hydrate laboratory.

Subtask 3.4 Construction of the Relative Permeability Data in Presence of Hydrate

Not initiated

Subtask 3.4 Identification of Hysteresis in Hydrate Stability

Not initiated

Task 4: Incorporation of Laboratory Data into Numerical Simulation Model

Subtask 4.1 Inputs and Preliminary Scoping Calculations

Not initiated

Subtask 4.2 Determination of New Constitutive Relationships

Continuing to the previous progress, we further showed that the new algorithm used in the previous quarterly report for capillary hysteresis is mathematically sound and numerically stable. Specifically, consider the following norm.

$$\|\chi\|_T^2 = \frac{1}{2}\int (p_g M_g^{-1} p_g + p_w M_w^{-1} p_w + \sigma_c \phi E_h^{-1} \sigma_c + \kappa \phi H_h^{-1} \kappa) d\Omega,$$

$$T := \left\{\chi := \left(p_g, p_w, \sigma_c, \kappa\right) \in R \times R \times R \times R : p_g, p_w, \sigma_c, \kappa \in L^2(\Omega)\right\},$$

where $\sigma_c = -p_c$ to have positive correlation between σ_c and S_w^t. Thus, E_h and H_h are positive, characterizing a capillary pressure curve. Then, the new algorithm provides

$$\frac{d}{dt}\left\|{}^d\chi\right\|_T^2 \le 0,\ \left\|{}^d\chi\right\|_T^{n+1} \le \left\|{}^d\chi\right\|_T^n,$$

which implies unconditional numerical stability (i.e., B-stability).

Subtask 4.3 Development of Geological Model

Not initiated

Task 5: Modeling of coupled flow and geomechanics in gas hydrate deposits

Subtask 5.1 Development of a coupled flow and geomechanics simulator for large deformation

We have been implementing the geomechanics module of large deformation in TOUGH+Hydrate, coupling two simulators. After implementation, we tested the enhanced simulator of T+M, comparing it with the previous study, Kim and Moridis (2012) in the 46th U.S. Rock Mechanics/Geomechanics Symposium. Specifically, we introduce a 2D reservoir with the plane strain geomechanics, placing a horizontal well located in the first hydrate layer at the left corner, shown in Fig. 5.1. We set the depth of the top zero (i.e., z=0). We take a scenario where a vertical fracture is created from the well down to the top of the underlying zone (i.e., -32~-48m in depth at x=0.25m). The hydrate and mud layers are located between -32m and -48 m in depth. Both layers have 0.25m thickness, being placed alternatively, and there are 64 layers in total.

From Fig. 5.2, we identified that the results between the previous and currently enhanced codes are identical, when deformation is small. This implies that the implementation of the enhanced codes is successful.

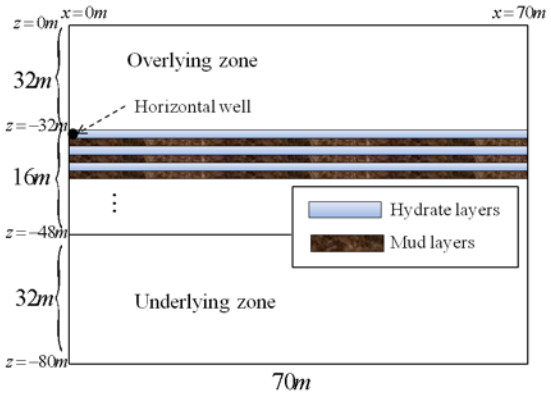

Fig. 5.1. 2D problem of gas production from the hydrate deposits by depressurization.

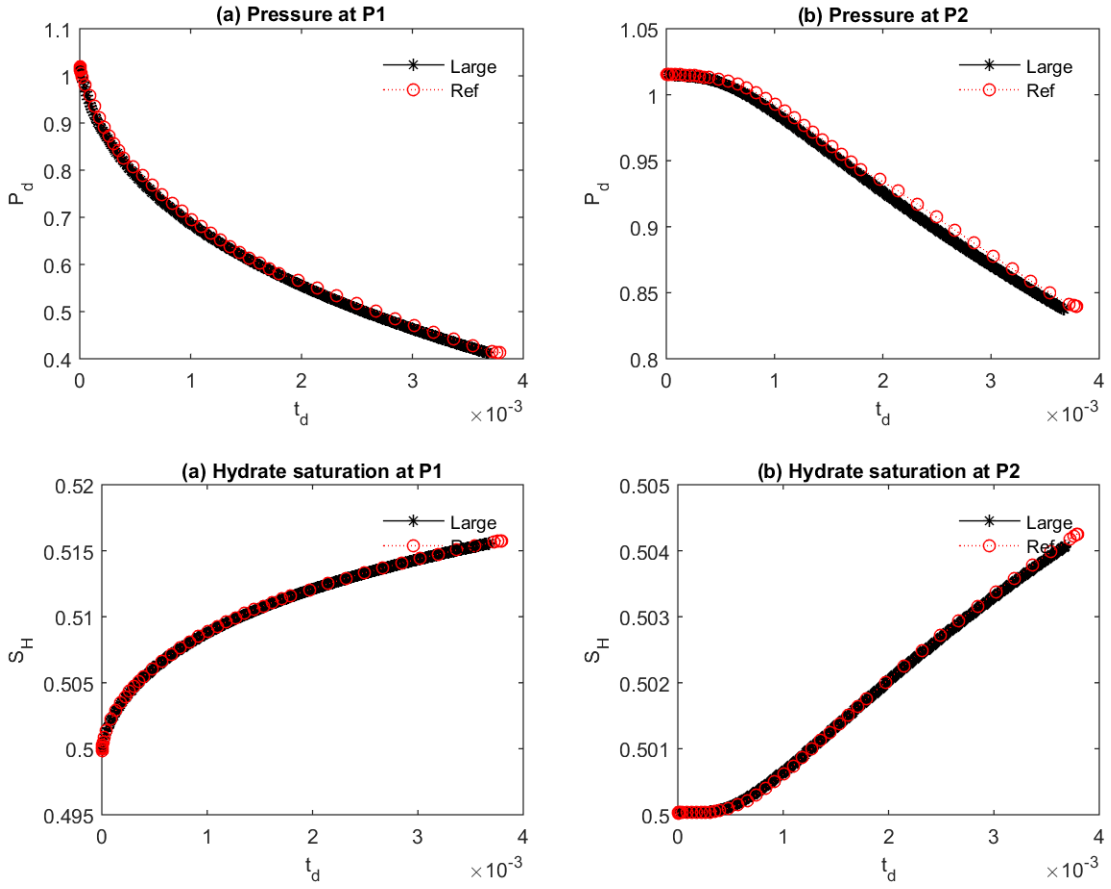

Fig. 5.2. We have two monitoring point of P1 at the well (0.25m, -32.125m) and P2 at (12m, -32.125m), located at the first hydrate layer. 'Ref" indicates the previous study based on assumption of small deformation, and 'Large' indicates the current enhanced simulator that can account for large deformation.

Subtask 5.2 Validation with experimental tests of depressurization

Not initiated

Subtask 5.3 Modeling of sand production and plastic behavior

Not initiated.

Subtask 5.4 Modeling of induced changes by formation of secondary hydrates: Frost-heave, strong capillarity, and induced fracturing

Following up on the discussion at the meeting of the 2nd International Code Comparison Study: Modeling THM Effects on Gas Production from Hydrate Bearing Reservoirs held in LBNL, we have been testing the mesh dependency on fracture propagation for frost-heave and induced fracturing. From Figs. 5.3 and 5.4, although the meshes are perturbed, we find that the different meshes still provide similar results of the direction of fracture propagation, not showing significant differences.

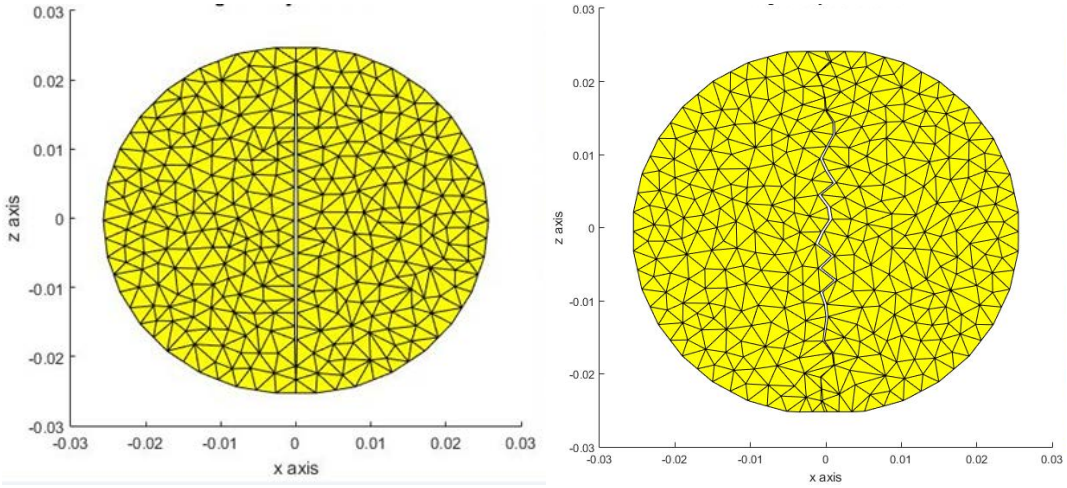

Fig. 5.3 Fractures from two different meshes for the Brazilian test.

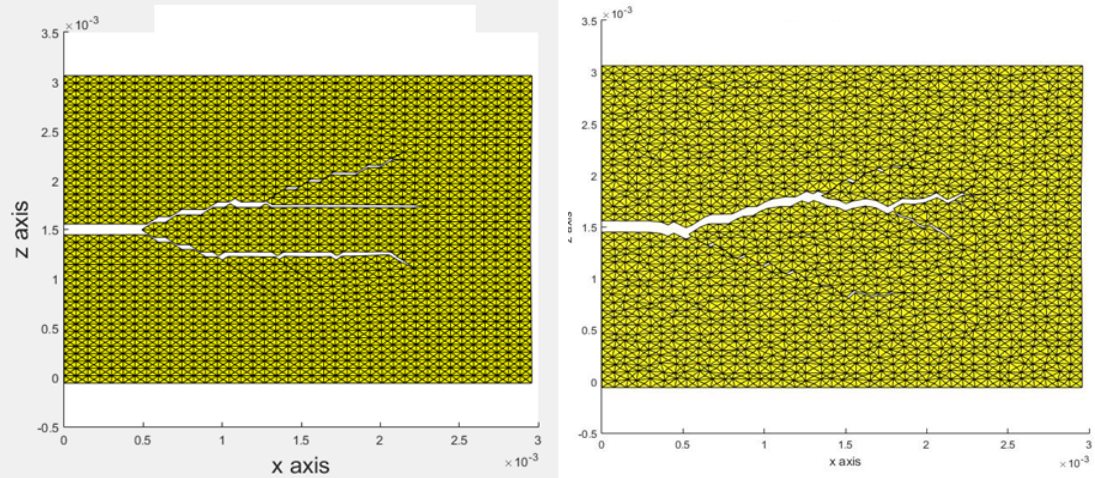

Fig. 5.4 Fracture propagations of the two different meshes for a tension test.

Subtasks 5.5 Field-scale simulation of PBU L106

Subtasks 5.6 Field-wide simulation of Ulleung Basin

For Subtasks 5.5 and 5.6, continuing to the previous progress, we have been testing capabilities (scalability and computational efficiency) of the parallel T+M for elastoplasticity. Elastoplasticity will be used for modelling wellbore instability of this project. We take a single producer, shown in Fig. 5.5, with a rate of 8 kg/s and the simulation time of 1095 days. The geomechanical properties are shown in Table 5.1.

Table 5.1—Material failure parameters

Parameter	Value
Initial pressure	30 MPa
Biot's coefficient	1.0
Young's modulus	0.6 GPa
Cohesion	3 MPa
Friction and dilation angles	0.52°
Thermal dilation coefficient	$4.5\times10^{-5\circ}\,\mathrm{C}^{-1}$

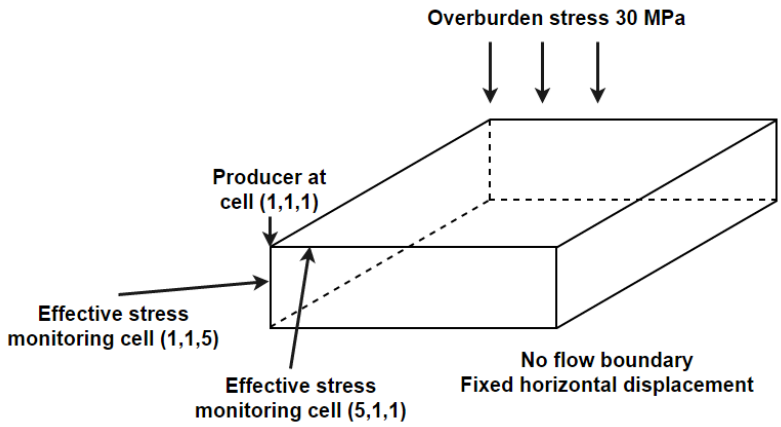

Fig. 5.5. Schematics of an elastoplastic coupled flow and geomechanics problem

For the load assignment, we distribute equal amount of continuous grid blocks to each process. In order to quantitatively represent the imbalance caused by plasticity, we define an idle-time ratio as $r_{id} = (t_{\max} - t_{\min}) / t_{\max}$, where t_{max} is the execution time of the process that has the heaviest return mapping load, and t_{min} is the execution time from process with the lightest return mapping load. The desirable case is $r_{id} = 0$, which implies that all processes are occupied fully and equally and no process needs to wait for others to finish return mapping computation. On the other hand, when $r_{id} = 1$, the work-load is assigned to processes unequally.

Table 5.2 shows the idle-time ratios at the first time step when no plasticity occurs, and the idle-time ratios at the 27th time step (395 days) when plasticity occurs at locations around the producer. The execution time used to calculate the idle time ratios does not include the message passing time, and the results shown here directly indicate the work load associated with certain processes.

At the first time step, the work load is balanced. As the process number becomes larger, the ratio increases. However, the execution time on each process becomes a few seconds as the process number becomes large, and even small difference of execution time can make the idle-time ratio significantly grow. At 395 days, the computation load for plasticity increases, resulting in the increment of idle-time ratios; some processes take predominantly elasticity while some processes experience plasticity. At 395 days, 44864 cells have plasticity computation. Thus, plasticity can lead to imbalance in the parallel environment. Smart assignment of processes is needed, considering areas of plasticity.

Table 5.2—Imbalance caused by return mapping process

	2 processes	4 processes	8 processes	16 processes	32 processes	64 processes

Idle-time ratios at first step	0.07%	1.52%	1.15%	1.25%	5.96%	14.09%
Idle-time ratios at 395 days	11.98%	12.48%	17.92%	25.32%	38.24%	46.67%

Task 6: Simulation-Based Analysis of System Behavior at the Ignik-Sikumi and Ulleung Hydrate Deposits

One PhD student has worked under the guidance of Drs. Akkutlu and Moridis and developed a numerical model of the sand packed cylinder using Tough+Hydrate version 1.5. This simulation model soon will be used to history-match the temperature and pressure data of the experiments and gain insight into the secondary hydrate formation. Note that the main role of the LBNL scientists will be to provide training, guidance and supervision of the numerical studies, the bulk of which will be conducted by TAMU graduate students. LBNL has initiated the training of a TAMU graduate student in the use of TOUGH+HYDRATE and ROCKMECH to support in this analysis.

PRODUCTS

We published three conference papers presented in the SPE reservoir simulation conference held in Montgomery, Texas, Feb. 20-23, as follows. The award of this project is acknowledged in the three following papers.

Guo X., Kim J., Killough J.E, 2017, Hybrid MPI-OpenMP Scalable Parallelization for Coupled Non-Isothermal Fluid-Heat Flow and Elastoplastic Geomechanics, 2017 SPE Reservoir Simulation Conference, 20-22 Feb., Montgomery, Texas, SPE-182665-MS

Yoon H.C., Zhou P., Kim J., 2017, Hysteresis Modeling of Capillary Pressure and Relative Permeability by using the Theory of Plasticity, 2017 SPE Reservoir Simulation Conference, 20-22 Feb., Montgomery, Texas, SPE-182709-MS

Yoon H.C., Kim J., 2017 The Order of Accuracy of the Fixed-Stress Type Two-Pass and Deferred Correction Methods for Poromechanics, 2017 SPE Reservoir Simulation Conference, 20-22 Feb., Montgomery, Texas, SPE-182664-MS

BUDGETARY INFORMATION

Table 2 shows the information of the budget for this project and the expenditure up to 03/31/2017.

Table 1 – Project timeline and milestones (Gantt Chart)

	FY17				FY18				FY19			
Quarter	Q1	Q2	Q3	Q4	Q1	Q2	Q3	Q4	Q1	Q2	Q3	Q4
Task 1.0. Project Management/Planning	A											
Task 2.0. Experimental study of gas hydrate in various scales for gas production of Ulleung Basin												
Subtask 2.1. Depressurization of 1 m scale in 1D				B								
Subtask 2.2 Depressurization of 10-m scale in 1D							C					
Subtask 2.3. Depressurization of 1.5-m scale in 3D										D		
Subtask 2.4. Revisit to the centimeter-scale system												
Task 3.0. Laboratory Experiments for Numerical Model Verification												
Subtask 3.1. Effective stress changes during dissociation				E								
Subtask 3.2. Sand production								F				
Subtask 33. Secondary hydrate and capillary pressure changes												G
Subtask 3.4. Relative Permeability Data												
Subtask 3.5. Hysteresis in Hydrate Stability												
Task 4.0. Incorporation of Laboratory Data into Numerical Simulation Model												
Subtask 4.1. Inputs and Preliminary Scoping Calculations									H			
Subtask 4.2. Determination of New Constitutive Relationships												
Subtask 4.3. Development of Geological Model												
Task 5.0. Modeling of coupled flow and geomechanics in gas hydrate deposits												
Subtask 5.1 Development of a coupled flow and geomechanics simulator for large deformation				I								
Subtask 5.2 Validation with experimental tests of depressurization										J		
Subtask 5.3 Modeling of sand production and plastic behavior								K				
Subtask 5.4 Frost-heave, strong capillarity, and induced fracturing												L
Subtask 5.5 Field-scale simulation of Ignik Sikumi/PBU L106												
Subtask 5.6 Field-wide simulation of Ulleung Basin												
Task 6.0. Simulation-Based Analysis of System Behavior at the Ignik-Sikumi and Ulleung Hydrate Deposits												M

Table 2 Budget information

Baselinie Reporting Quarter	Budget Period 1							
	Q1		Q2		Q3		Q4	
	10/01/16-12/31/16		01/01/17-03/31/17		04/01/17-06/30/17		07/01/17-09/30/17	
	Q1	Cumulative Total	Q2	Cumulative Total	Q3	Cumulative Total	Q4	Cumulative Total
Baselinie Cost Plan								
Federal (TAMU)	$37,901	$37,901	$57,809	$95,711	$43,967	$139,678	$34,206	$173,884
Federal (LBNL)	$18,750	$18,750	$18,750	$37,500	$18,750	$56,250	$18,750	$75,000
Non-Federal Cost Share	$6,986	$6,986	$6,986	$13,972	$6,986	$20,958	$656,986	$677,944
Total Planned	$63,637	$63,637	$83,545	$147,183	$69,703	$216,886	$709,942	$926,828
Actual Incurred Cost								
Federal (TAMU)	$0	$0	$7,602.38	$7,602				
Federal (LBNL)	$0	$0	$0	$0				
Non-Federal Cost Share	$0	$0	$6,986	$6,986				
Total incuured cost	$0	$0	$14,588.38	$14,588				
Variance								
Federal (TAMU)	($37,901)	($37,901)	($50,207)	($88,108)				
Federal (LBNL)	($18,750)	($18,750)	($18,750)	($37,500)				
Non-Federal Cost Share	($6,986)	($6,986)	$0	($6,986)				
Total variance	($63,637)	($63,637)	($68,957)	($132,594)				

Baselinie Reporting Quarter	Budget Period 2							
	Q1		Q2		Q3		Q4	
	10/01/17-12/31/17		01/01/18-03/31/18		04/01/18-06/30/18		07/01/18-09/30/18	
	Q1	Cumulative Total	Q2	Cumulative Total	Q3	Cumulative Total	Q4	Cumulative Total
Baselinie Cost Plan								
Federal (TAMU)	$42,481	$42,481	$35,307	$77,788	$46,367	$124,155	$39,908	$164,063
Federal (LBNL)	$18,750	$18,750	$18,750	$37,500	$18,750	$56,250	$18,750	$75,000
Non-Federal Cost Share	$6,986	$6,986	$6,986	$13,972	$6,986	$20,958	$6,986	$27,944
Total Planned	$68,217	$68,217	$61,043	$129,260	$72,103	$201,363	$65,644	$267,007
Actual Incurred Cost								
Federal (TAMU)								
Federal (LBNL)								
Non-Federal Cost Share								
Total incuured cost								
Variance								
Federal (TAMU)								
Federal (LBNL)								
Non-Federal Cost Share								
Total variance								

Baselinie Reporting Quarter	Budget Period 3							
	Q1		Q2		Q3		Q4	
	10/01/18-12/31/18		01/01/19-03/31/19		04/01/19-06/30/19		07/01/19-09/30/19	
	Q1	Cumulative Total	Q2	Cumulative Total	Q3	Cumulative Total	Q4	Cumulative Total
Baselinie Cost Plan								
Federal (TAMU)	$43,543	$43,543	$36,189	$79,733	$47,526	$127,259	$41,209	$168,468
Federal (LBNL)	$18,750	$18,750	$18,750	$37,500	$18,750	$56,250	$18,750	$75,000
Non-Federal Cost Share	$6,986	$6,986	$6,986	$13,972	$6,986	$20,958	$6,986	$27,944
Total Planned	$69,279	$69,279	$61,925	$131,205	$73,262	$204,467	$66,945	$271,412
Actual Incurred Cost								
Federal (TAMU)								
Federal (LBNL)								
Non-Federal Cost Share								
Total incuured cost								
Variance								
Federal (TAMU)								
Federal (LBNL)								
Non-Federal Cost Share								
Total variance								